5

2 C
5

OTS: 60-11,344

JPRS: 2308

26 February 1960

SELECTED TRANSLATIONS ON

SOVIET SPACE RESEARCH

Distributed by:

OFFICE OF TECHNICAL SERVICES
U. S. DEPARTMENT OF COMMERCE
WASHINGTON 25, D. C.

~~Price: $0.75~~

U. S. JOINT PUBLICATIONS RESEARCH SERVICE
205 EAST 42nd STREET, SUITE 300
New York 17, N. Y.

JPRS: 2308

CSO: 3138-N/a

ON THE PROBLEM OF INVESTIGATING ATMOSPHERIC OZONE BY PHOTOMETRY OF LUNAR ECLIPSES

V.G. Fesenkov

Astronomicheskiy Zhurnal
[Astronomical Journal],
Vol. XXXVI, No.4, Moscow,
Jul.-Aug. 1959, pp.564-572

Together with a presentation of the theoretical foundation of this phenomenon, the illumination during different phases of a lunar eclipse are calculated for a standard terrestrial atmosphere without ozone, as well as for the varying distribution of ozone depending on altitude above sea level. The results are summarized in table 3. This table contains: 1) the different limiting heights in the atmosphere illuminated by passing solar rays, as this appears from the moon; 2) the corresponding phase angles for the observed area of the moon, i.e. the angular distance of the area from the center of the earth's umbra; 3) the illumination J/J_0 for $\lambda=0.5\ \mu$, calculated for a standard atmosphere without ozone in units of illumination produced by the uneclipsed sun; 4) and 5) the same as 3) but for an ozone admixture with a total vertical depth equal to 0.031 and at heights of 21 and 26 km, respectively; 6) and 7) the absorption produced by ozone under these conditions expressed in stellar magnitudes.

An inspection of photometric curves, similar to those in figs. 2-6, indicates that it is possible to determine the distribution of atmospheric ozone on the basis of altitude, as well as its

total content in the atmosphere.

During lunar eclipses diverse regions on the moon are illuminated by solar rays which simultaneously pass through different layers of the earth's atmosphere. This illumination may be computed theoretically by assuming a certain standard condition of the earth's atmosphere. Any admixture in the atmosphere's high layers of foreign absorbing particles incapable of changing the direction of the solar rays, as well as the occurrence of a certain amount of ozone may be discovered by photometric measurements made in different wave lengths during various phases of the eclipse.

To facilitate such calculations it is desirable to have tables at hand which represent the trajectories of solar rays which pass directly through the earth's atmosphere at diverse minimum altitudes h_o above sea level.

Let there be for each parameter of h_o at the polar coordinates r and φ, considered from the center of the earth, the relation

$$r = f(\varphi, h_o),$$

as well as the corresponding expression for refraction

$$Refr = F(\varphi, h_o),$$

where the amplitude angle φ is taken from the direction of the initial vector. The accuracy of these magnitudes for r and Refr depends entirely on the value of the refractive index n at different altitudes.

We have, with sufficient accuracy,

$$n = 1 + c\rho ,$$

where ρ is the air density. The constant c depends on λ. The relations may be found, as this has been shown in detail in (1), through the series representing the radius vector as a function of the amplitude angle by means of the so-called coefficients of refraction. To determine the refraction it is also possible to use a similar series, although the accuracy will then be considerably reduced, due to the fact that this has essentially to be derived from the amplitude angle which lowers convergence considerably. However, since the value of refraction between the point of greatest approach of the trajectory to the earth's surface at altitude h_o and the given vector is

$$Refr = \zeta + \varphi - 90^o ,$$

whereupon

$$\operatorname{ctg} = \frac{1}{r}\frac{dr}{d\varphi}, \qquad , \qquad (1)$$

it appears simpler, instead of using the series, to employ the fundamental refraction equation with the known form

$$rn \sin\zeta = r_0 n_0 \sin\zeta_0 \qquad . \qquad (2)$$

Knowing r as a function of φ, we find ζ from this and then the corresponding Refr. It is also possible to directly determine the trajectory of the light ray passing through the entire atmosphere by means of an equation described in the form of an integral in which the radius vector is a variable.

Actually, excluding angle ζ from relations (1) and (2), we obtain

$$\varphi = \int_{\frac{r_0}{r}}^{1} \frac{\frac{n_0}{n} d\left(\frac{r_0}{r}\right)}{\sqrt{\operatorname{ctg}^2\zeta + 1 - \left(\frac{r_0 n_0}{rn}\right)^2}} \qquad .$$

This equation may be used conveniently to compute the trajectory of the light beam, only if ζ_0 differs from 90° and, hence, the denominator is not reduced to zero at any one of its points.

Besides, starting out from (2), angle ζ may be represented in the form

$$\zeta + \text{const} = \int \frac{d\left(\frac{r_0}{r}\frac{n_0}{n}\right)}{\sqrt{\operatorname{ctg}^2\zeta_0 + 1 - \left(\frac{r_0 n_0}{rn}\right)}} \qquad .$$

Taking into consideration that angle is reduced to zero at infinity when $r = \infty$, and noting that for the initial point of the trajectory

$$\zeta = \zeta_0; \quad r = r_0; \quad n = n_0 \quad ,$$

we find

$$\zeta_0 = \int_0^1 \frac{n_0}{n} \frac{d\left(\frac{r_0}{r}\right)}{\sqrt{ctg^2\zeta_0 + 1 - \left(\frac{r_0 n_0}{r n}\right)^2}} + \int_{h_0}^1 \frac{r_0}{n} \frac{d\left(\frac{n_0}{n}\right)}{\sqrt{ctg^2\zeta_0 + 1 - \left(\frac{r_0 n_0}{r n}\right)^2}}$$

The first integral on the right side of this equation represents the amplitude angle φ, taken between the initial and infinitely distant points on the light trajectory which is equal to the true zenith distance of the luminary ζ_1, that it has in the absence of refraction. On the other hand, ζ_0 is the apparent zenith distance at the initial point of the trajectory. Refraction throughout the entire range of the light beam is, apparently, the difference

$$\text{Refr} = \zeta_1 - \zeta_0$$

and, consequently,

$$\text{Refr} = \int_1^{n_0} \frac{\frac{r_0}{r} d\left(\frac{n_0}{n}\right)}{\sqrt{ctg^2\zeta_0 + 1 - \left(\frac{r_0 n_0}{r n}\right)^2}} \quad .$$

The refraction between the original and any intermediate points in the trajectory is evidently,

$$\text{Refr} = \int_1^{\frac{n_0}{n}} \frac{\frac{r_0}{r} d\left(\frac{n_0}{n}\right)}{\sqrt{ctg^2\zeta_0 + 1 - \left(\frac{r_0 n_0}{r n}\right)^2}} \quad .$$

In order to avoid singularity in the integrand for the initial point in the trajectory, computations may be made from its terminal point upon escape from the atmosphere, making the radius vector large enough and assuming the refractive index is equal to unity. In any case, the computation of the light trajectories which pass through the terrestrial atmosphere at different altitudes above the earth's surface does not present any difficulty. Appropriate tables, which we have figured out for 0.5 μ wave length, are given in (1).

The determination of the extinction coefficient which corresponds to each element in the light beam trajectory is incomparably more difficult, inasmuch as this is related to diverse admixtures in the gas medium at different altitudes, and the proportion of these admixture:

is far from constant. It may be assumed that the content of very fine dust increases with altitude, although water pairs occur in completely insignificant quantities beyond the troposphere. It may nevertheless be assumed for the standard atmosphere without ozone that the coefficient of absorption k in the expression

$$d\tau = k\rho\, dh$$

is a constant value, so that

$$\tau = k\int \rho\, dh .$$

This coefficient may be determined by the transparency of the atmosphere, known from observation

$$p = e^{-\tau}$$

All other factors, as, for instance, ozone or cosmic dust, if such exists in the high layers of the atmosphere, produce a certain deviation from standard conditions and may be differentiated by pertinent observations during lunar eclipse.

We will imagine that there is a hypothetical observer on the surface of the moon at the time of an eclipse.

For this observer each element of the solar disk

$$d\sigma = r\, dr\, d\varphi$$

is visually transposed by the action of double refraction to the immediate vicinity of the visible limb of the earth and is transferred to the extraordinarily compressed element

$$d\sigma' = \rho\, d\rho\, d\varphi ,$$

where $\rho = R + h_o$.

All values which enter the picture here are expressed in the very same angular units. The corresponding double refraction, known from the table, as a function of h_o is

$$2\ \mathrm{Refr} = \rho - r = R + h_o - r .$$

The illumination of a particular area on the moon is determined by integration of all the elements of the solar disk, expressed by the equation

$$J = 2\int_{d-\delta_0}^{d+\delta_0} r\,dr \int_0^{\varphi_{max}} \frac{d\sigma'}{d\sigma}(ext)\, j\left(\frac{\delta}{\delta_0}\right) d\varphi \qquad (3)$$

where d is the angular distance between the centers of the earth and sun seen from a given region on the moon, δ_0 - is the solar radius in the same angular measure, $j\left(\frac{\delta}{\delta_0}\right)$ - is the distribution of brightness on the solar disk, (ext) - is extinction.

We have found through obvious considerations that

$$\cos\varphi_{max} = \frac{r^2 + d^2 - \delta_0^2}{2dr} \quad \text{and} \quad r\frac{d\sigma'}{d\sigma} = \frac{R + h_0}{1 - \frac{d(2R_{refr})}{dh_0}}.$$

Passing from h_0 expressed in angular measure to the linear value expressed, for instance, in kilometers and deriving from double refraction according to its absolute value, we find that

$$1 - \frac{d(2R_{refr})}{dh_0} = 1 + b\left|\frac{d(2R_{refr})}{dh_0}\right|,$$

l - is the distance between the moon and earth.

The latter equation accurately represents the weakening in illumination from the sun, as a result of the dispersion of rays which pass through the non-homogeneous medium of the earth's atmosphere with a gradual lessening in the curvature of the rays at a greater distance from the earth's surface.

Hence, when atmospheric extinction is lacking, the apparent brightness of the solar image, transformed by the earth's atmosphere, as seen by an observer on the moon, remains identical to that without an eclipse.

This same effect, although to an incomparably lesser extent, also exists for an observer situated directly on the surface of the earth when the the sun passes close to the horizon. Since this effect does not depend on the angular dimensions of the object, it should be taken into consideration for stars as well, acting toward an increase in ordinary atmospheric extinction.

With the intention of investigating diverse admixtures to the standard atmosphere, how these appear at the different altitudes h_0, it is more expedient to write equation (3) in an equivalent form, integrating with h_0 instead of r. In accordance with this, for actual calculation, one assumes the expression

$$J = 2\int_{d-\delta_0}^{d+\delta_0} (R+h_0)(ext)\,dh_0 \int_0^{\varphi_{max}} j\left(\frac{\delta}{\delta_0}\right) d\varphi \qquad (4)$$

where

$$(ext) = e^{-\tau}.$$

τ - is the optical depth of the entire atmosphere along the pertinent horizontal ray which passes above the terrestrial surface at the minimum height h_0.

Illumination, represented by equation (4), should be referred to the illumination which is produced by the sun on the same region of lunar surface without an eclipse. To do this, the values which have been found should be differentiated as

$$J_0 = 2\pi \int_0^1 \frac{\delta}{\delta_0}\, j\left(\frac{\delta}{\delta_0}\right) d\frac{\delta}{\delta_0} \cdot \delta_0^2 \qquad (5)$$

where $j\left(\frac{\delta}{\delta_0}\right)$ indicates, just as before, the distribution of intensity on the sun's disk.

The extinction of horizontal rays and corresponding refractive dispersion reduce the luminosity of the moon during eclipse to an extremely high degree. In all actuality, during the full lunar eclipse only a very small part of the sun's disk (near the limb of the earth) is of real importance. Close to the end of full phase the active portion of the atmosphere which appears illuminated to the moon viewer incessantly increases with the approach of the sun to the earth's limb, encompassing ever greater heights, while the inside section of the deformed image of the sun remains practically bound to these same low air layers.

In the simplest particular instance, corresponding to the central phase of the full eclipse, where d equals zero, and the entire event is distinguished by complete symmetry, each circular ring into which the solar disk could be divided yields two images for the hypothetical observer on the moon. The most extreme ring which corresponds

to the external contour of the solar disk assumes the form of the thinnest annulus, encircling the entire earth and is visible at an altitude of 5.56 km, and at the same time the shape of a weaker ring, visible at a height of 1.55 km.

Every other concentric zone in the center of the solar disk also produces two images, so that in the final reckoning the whole solar disk is situated between the indicated limits, appearing as a dense ring with a total visible width of only 2.5", the brightness of which falls rapidly according to the degree of proximity to the earth's limb.

It follows from this that the solid angle under which the sun appears from the moon dwindles at the momentof the eclipse's central phase to a negligibly small fraction, namely approximately 70 times less than the initial value, meanwhile including together with this the effect of dispersion which was mentioned above.

To perform needed computations, we have compiled an auxiliary table according to argument h_0, giving $R + h_0$, furthermore the horizontal double refraction, the radius vector r, whereupon the corresponding element in the solar disk is taken visually up to the level of the given layer of atmosphere, and finally, the degree of transparency e^{-2} for the given trajectory. The radius of the earth's disk is taken at 57.6. In further calculations the radius of the solar disk is assumed to be equal to 16' (see table 1).

TABLE 1

h_0	h'_0	$R + h_0$	2Refr	r	$e^{-2\tau}$
1	2	3	4	5	6
5 км	0'045	57'645	45'190	12'555	0.382×10^{-4}
10	0.090	57.690	24.180	33.510	0.729×10^{-3}
15	0.136	57.736	8.995	48.741	0.1083
17.5	0.159	57.759	6.099	51.660	0.224
20	0.181	57.781	3.819	53.962	0.361
22.5	0.204	57.8035	2.474	55.330	0.498
25	0.226	57.826	1.706	56.120	0.625
27.5	0.249	57.848	1.208	56.640	0.729
30	0.271	57.871	0.800	57.071	0.805
35	0.316	56.916	0.400	57.516	0.901
40	0.362	57.962	0.200	57.762	0.956
45	0.407	58.007	0.100	57.907	0.976
50	0.452	58.052	0.050	58.002	0.988
55	0.497	58.097	0.025	58.072	0.994
60	0.542	58.142	0.012	58.130	0.998
65	0.587	58.187	0.006	58.181	1.000
70	0.633	58.233	0.003	58.230	1.0
75	0.678	58.278	0.0015	58.277	1.0
80	0.724	58.324	0.00075	58.323	1.0
85	0.769	58.369	0.00038	58.369	1.0
90	0.814	58.414	0.00019	58.414	1.0
100	0.904	58.504	0.00005	58.504	1.0
110	0.994	58.594	0.00	58.594	1.0
120	1.084	58.684	0.00	58.684	1.0
125	1.130	58.730	0.00	58.730	1.0
150	1.356	58.956	0.00	58.956	1.0
175	1.582	59.182	0.00	59.182	1.0
200	1.808	59.408	0.00	59.408	1.0
250	2.260	59.860	0.00	59.860	1.0
300	2.712	60.312	0.00	60.312	1.0
350	3.164	60.764	0.00	60.764	1.0
400	3.616	61.216	0.00	61.216	1.0
800	7.232	64.832	0.00	64.832	1.0

In order to take the effect of ozone into consideration for any particular wave length, it is first of all necessary to estimate the optical depth for the respective trajectories of the solar rays. Two characteristic cases are examined. Assuming the distribution of ozone in relation to altitude to be in accordance with Laplace's formula

$$C = Ae^{-\alpha (h - h_1)^2},$$

we take the height of maximum concentration h_1 as 21 and 26 km respectively. Coefficient α is assumed equal to 0.0283, which corresponds to a four-fold drop in ozone concentration every 7 km in altitude (see (2)).

The optical depth for the horizontal trajectories is computed according to the usual expression

$$\int C \sec \zeta \, dh,$$

which is equivalent to the following

$$[\tau_0 = \cdot [A] \int e^{-\alpha (h-h_1)^2} \frac{(R+h)\varphi}{\cos(\varphi - R\varphi_1)}$$

Coefficient A is determined by comparing its value with the optical depth along the vertical, assumed equal to 0.031 for $\lambda = 0.5\ \mu$. The transparency $e^{-\tau_0}$ for ozone, computed in a similar manner for different horizontal trajectories which correspond to the total range at h_0, is presented in table 2. As may readily be seen, this indicates the characteristic path at altitude h_0, and is strongly reminiscent of the Götz reverse effect. Transparency in the ozone is not very low precisely at the lowest layers, further dropping with altitude, and upon reaching the minimum somewhat below the height of maximum concentration rapidly increases right up to unity. In essence, both curves which represent transparency in the ozone are completely identical and distinguishable from one another solely by a shift in altitude at 5 km (see table 2).

Table 2

h_0	$e^{-\tau_0}$ h_1=21 km	$e^{-\tau_0}$ h_1=26 km	h_0	$e^{-\tau_0}$ h_1=21 km	$e^{-\tau_0}$ h_1=26 km
0 km	0.442	—	20	0.186	0.202
2.5	0.426	—	22.5	0.328	0.180
5	0.400	0.442	25	0.517	0.198
7.5	0.366	0.426	27.5	0.747	0.324
10	0.312	0.369	30	0.924	0.519
12.5	0.252	0.305	35	0.999	0.925
15	0.188	0.315	40	1.000	0.999
17.5	0.160	0.244			

The data in this table are represented by the curves in figure 1. Actually, both curves characterizing transparency in the ozone for different horizontal trajectories are nearly precisely marked by parallel paths.

In this manner, rather extensive computations have been made for the different angles d which essentially represent the angular distances between the centers of the earth's shadow and the observed area on the lunar disk. Figures 2,3, and 4 show values of the integrand functions (4) taken according to the argument h_o for three characteristic values of the angles at d, namely immediately after the end of the full phase of the eclipse, corresponding to d = 41'.6, when the solar limb seen from the moon reaches an altitude h_o at 40.70 and 400 km respectively (d = 41'.96; 42'.23; 45'.22).

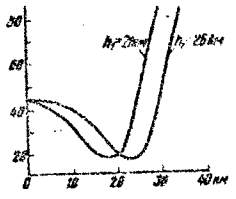

Рис. 1

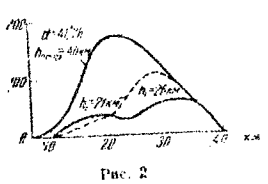

Рис. 2

In these drawings the upper curve represents the value of the integrand function for a standard atmosphere with density distribution according to altitude in conformity with (2). The point curve refers to ozone content, shown above, with the maximum concentration at an altitude of 21 km; the thin solid curve refers to the same ozone content, although with a maximum concentration displaced 5 km higher, i.e. up to 26 km.

As may be seen, even a small admixture of ozone has an extraordinarily strong effect on the luminosity of the moon's surface during an eclipse. Even at the maximum value of h_o at 70 km, the influence of ozone is still perceived extremely strongly, gradually lessening however, as further transition into the penumbra occurs. It is apparent, besides, from the illustrations presented that a slight shift in the altitude of maximum ozone concentration exerts a very perceivable effect on the general illumination in the corresponding wave length. Even at h_o equal to 400 km, where the influence of the lower layers of the atmosphere makes itself very much negligible in terms of general illumination, exact measurements may disclose a discrepancy in the corresponding distribution of ozone according to altitude.

All the numerical findings which have been gathered are summarized in table 3.

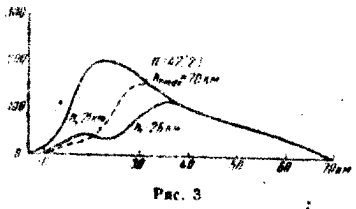

Рис. 3

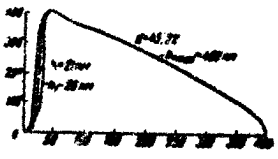

Рис. 4

Fig. 3 Fig. 4

Table 3

1	2	4	5	6	7	
10	20.51	1.86·10⁻³	h_3 = 21 km: 0.651·10⁻⁷	h_3 = 26 km: 0.772·10⁻⁷	h_3 = 21 km: 1.138	h_3 = 26 km: 0.950
20	37.46	2.70·10⁻³	0.55·10⁻⁴	0.650·10⁻⁴	1.478	1.071
30	49.12	5.79·10⁻³	1.28·10⁻⁴	1.423·10⁻⁴	1.642	1.524
35	51.17	1.044·10⁻²	0.331·10⁻³	0.253·10⁻³	1.497	1.764
40	51.76	1.618·10⁻²	0.827·10⁻³	0.577·10⁻³	0.765	1.157
50	52.23	3.015·10⁻²	2.195·10⁻³	1.758·10⁻³	0.392	0.588
100	52.50	5.43·10⁻²	4.688·10⁻³	4.062·10⁻³	0.212	0.315
200	52.61	1.460·10⁻²	1.513·10⁻²	1.314·10⁻²	0.107	0.108
400	52.62	3.257·10⁻²	3.284·10⁻²	3.302·10⁻²	0.027	0.045
800	52.62	0.190	0.156	0.158	0.015	0.015

This table contains: 1) limiting altitudes in the atmosphere which are still illuminated by passing solar rays; 2) the corresponding phase angles for the observed regions on the moon, i.e. the angular distances of this area from the center of the terrestrial umbra; 3) the illumination J/J_0 for $\lambda = 0.5$ μ, computed for a standard atmosphere taken without ozone and expressed in units of illumination from the uneclipsed sun; 4) and 5) are similar illuminations for ozone with full vertical optical depth, equal to 0.031, and with heights of maximum concentration at respectively 21 and 26 km; 6) and 7) are corresponding absorptions in stellar magnitudes, produced by ozone. The data given in these tables make it possible to trace photometric singularities in the lunar eclipse, both for a standard atmosphere without ozone and also with ozone, distributed in diverse manners. Were observations to be made in wave lengths where the influence of the ozone absorption band is insignificant, as, for instance, in the blue or extreme red light rays, and a photometric curve is plotted on the basis of these observations for the intermediate part of the spectrum, where the effect of the Shapyui [?] absorption band appears, it would be possible, by comparing a similar neutralized curve with the actually observed one for this part of the spectrum to deduce the effect of ozone at the pertinent wave length and thus at different phases of an eclipse.

The findings will be similar to those shown on the basis of the data in table 3 in fig. 5. As may be seen, even absorption in such a weak band as the Shapyui band at a wave length of 0.5 μ attains values, for those horizontal rays which penetrate the earth's atmosphere, up to 1.8 stellar magnitudes, and, moreover, to a considerable

extent depends on the distribution of ozone according to altitude. As pointed out above, the maximum altitudes of $h_\odot$, still illuminated by the sun, are directly related to the phase of the eclipse d.

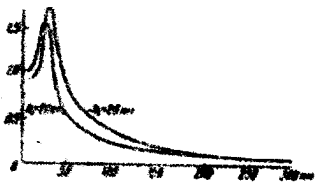

Fig. 5

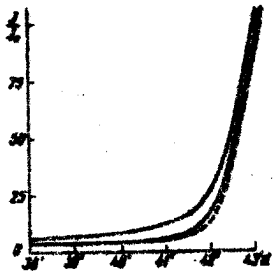

Fig. 6

Finally, the general photometric curves are depicted in figure 6 which show the course of illumination of the area on the moon during the phase of the eclipse for all three cases indicated above (the standard atmosphere without ozone and the same atmosphere with the presence of ozone, distributed diversely according to altitude).

Evidently, within a full phase of an eclipse the illumination of the lunar surface slowly and gradually increases by the sun's approach to the limb of the earth, as seen from the moon. Further on, upon transition to the penumbra, the illumination rapidly begins to grow. The point in the photometric curve which corresponds to its maximum slope is perceived by the viewer as the edge of the earth's shadow. It is immediately apparent from this that the visible dimensions of the earth's shadow are noticeably greater than the theoretical values, determined by the inside contact of the sun with the limb of the earth's disk. This has actually been confirmed by all observers. The corresponding increase may be estimated at 0'.03 for the standard atmosphere lacking ozone, and

at 0'.1 - 0'.2% for the real atmosphere with ozone. Generally speaking, the admixture of ozone in the upper layers of the atmosphere may perceptibly increase the size of the earth's shadow. As a result of this, it would be most expedient to measure the dimensions of the earth's shadow during eclipse, even if this is during the time the edge of the shadow passes through diverse lunar details, provided that such measurements are made simultaneously in different spectral bands which correspond to absorption in ozone and without it.

The theoretical computations explained above graphically show the possibility of determining both the total content of ozone in the atmosphere and its distribution according to altitude from photometric observations made in different wave lengths and the corresponding various eclipse phases, especially near the edge of the umbra upon its transition to the penumbra.

Together with this, these computations indicate that it is absolutely unthinkable, as this has been done by various authors, to neglect the angular dimensions of the sun, i.e. to consider that the illumination of the lunar area during each given phase is determined by solar rays which pass solely along a single determined trajectory. On the contrary, this illumination is determined by the light paths which pass through at a wide range of altitudes.

Institute of Astrophysics
Academy of Sciences, Kazakh SSR

Submitted to
the editorial
offices
1 June 1959

Bibliography

1. V.G. Fesenkov, Astron. zh. [Astronomical Journal], 36, vyp. 2, 1959.

2. Ch. Allen, Astrophys. Quantities, London, 1955.

CSO: 3138-N/b

MEAN HOURLY NUMBER OF METEORS RECORDED BY A RADAR SET

I. STREAMS

Ye.I. Fialko

Astronomicheskiy Zhurnal
[Astronomical Journal],
Vol. XXXVI, No.4, Moscow,
Jul.-Aug.1959, pp.626-628

A general expression is given for the number of meteors detected by a radar set during normal reflection (scattering) of radio waves by an ionized trail in the case of a stream. A simplified workable formula has been derived.

The problem of the number of meteors registered has been examined in diverse works (1-4), etc.

However, it is necessary to treat more completely and accurately the relation between the findings of radar observations (according to number) and the parameters of the meteors, atmosphere and radar equipment.

1. THE DEPENDENCE OF THE NUMBER OF REGISTERED METEORS ON THE PARAMETERS OF THE RADAR SET AND CHARACTERISTICS OF THE METEOR AND ATMOSPHERE

The quantity of meteoric bodies with masses in the interval $m \div m + \Delta m$ which pass per unit time through a unit area, the normal path of the meteor, is equal (2) to

$$\Delta N = f(m)\,\Delta m. \tag{1}$$

The number of meteors in a stream fixed for an observation time $t_1 \div t_2$ in the interval of altitudes $h_1 \div h_2$ lying in the sector $\theta_1 \div \theta_2$ of the echo's plane (2), as it is easy to show in the case of normal radio wave reflection, will be equal to (fig. 1)

$$N = \int_{t_1}^{t_2} \frac{dt}{\sin^3\chi} \int_{\theta_1}^{\theta_2} \frac{d\theta}{\cos^2\theta} \int_{h_1}^{h_2} h\,dh \int_{m_{min}}^{\infty} f(m)\,dm \tag{2}$$

where χ - is zenith distance of the stream's radiant; θ - is the angle and plane of the echo reckoned from a certain direction (for example, axially); m_{min} - is the minimum mass of a meteoric body which creates an ionized trail detected by radar, equal to (2)

$$m_{min} = \left(\alpha_{min}^{1/2} \sqrt{\frac{\xi \mu H}{\beta p}} + \frac{pv^2}{3 Q e \pi \lambda}\right)^3 \tag{3}$$

H and p - are the altitude of the homogeneous atmosphere and the atmospheric pressure in a section of normal radio wave reflection; v - is the velocity of the meteor; β - is the probability of ionization; μ - is the mass of an atom in the meteoric body; Q - is the coefficient characterizing the physical properties and geometrical peculiarities of the meteoric body (2); α_{min} - is the minimum registrable linear density of the electrons, equal to (5)

$$\alpha_{min} = B \sqrt{\frac{\xi_{por} R^3 \lambda^2}{P_1 \lambda^3 G}} \frac{\Delta^{0.5}}{1 - e^{-4.5\Delta^{0.5}}} e^{(2\pi/\lambda)^2 (a^2 + 4 D T_{min})}, \tag{4}$$

where ξ_{por} - is the power of the receiver signal threshold; R - is the slant range from locator station to the meteor track; P_1 - is the radiated power in a pulse; λ - is the wave length; G - is the directive gain of the antenna; $B = 8.10^{13}$ elec/cm; α - is the initial radius of the meteoric trail; D - is the diffusion factor (at the point of radio wave reflection); T_{min} is the minimum time necessary for registration, during which the echo signal should exceed the threshold level;

$$\Delta = \frac{16\pi^2 D R^{1/2}}{v \lambda^{3/2}} \tag{5}$$

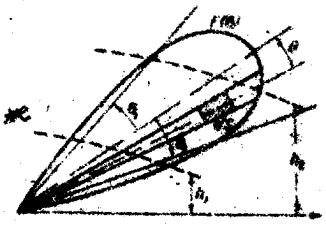

Fig. 1. The echo plane: F (θ) - is a diagram of the directivity of emission in the echo plane; h - is the altitude above the earth's surface; dS - is the echo plane element

The differential law of mass distribution of meteoric bodies is ordinarily written in the form (2,6):

$$f(m) = \frac{b}{m^s}, \qquad (6)$$

where b and s - are constants.

It follows from (2) and (6) that the number of registered meteors in the stream may be represented in the form:

$$N = \frac{b}{s-1} \int_{t_1}^{t_2} \frac{dt}{\sin^2 \chi} \int_{\theta_1}^{\theta_2} \frac{d\theta}{\cos^2 \theta} \int_{h_1}^{h_2} dh \, dh \, \frac{1}{m_{min}^{s-1}}, \qquad (7)$$

where m_{min} is determined from (3) and (4).

Expressions (7), (3) and (4) characterize the dependence of the observation (according to number) on the parameters of the meteor, atmosphere and radar equipment in the case of a stream.

2. A PARTICULAR CASE (RECEPTION FROM A SMALL SPACING OF ALTITUDES IN A NARROW SECTOR)

The most intensive ionization occurs in the zone with characteristic altitude h_m(2). It is for this reason that an examination of a particular case, the reception of echo signals from the thin layer region lying at an altitude of $h \approx h_m$ with a small aperture in sector $\Delta\theta$ (in the echo plane).

In this case the pressure was equal to (2)

$$p \approx p_m = \frac{Q \alpha_m \lambda}{\nu^2} m^{5/2} = \frac{2\gamma Q'}{\nu\lambda}\left(\frac{q}{4} H \alpha_m \cos^2\chi\right)^{5/2} \qquad (8)$$

where α_m - is the linear density of the electrons which corresponds to the characteristic altitude; $Q = 2l\,g/\Lambda A$; $Q' = l\,(\lambda A)^{-1}(\mu/\beta)^{\frac{1}{3}}$; l - is the latent heat of steam formation; Λ - is the heat transfer factor (2,6); $A = A_0/\delta^{2/3}$ - is the coefficient of meteoric body form; δ - is the density of the meteoric body; A_0 - is the coefficient dependent on the form of the body; in the case of a sphere, $A_0 = 1.21$ (6).

After conversion formula (7) takes the form (for the instance of a short observation interval $\Delta t = t_2 - t_1$):

$$N \approx \frac{b\,\Delta t\,\Delta\theta\,(h_\lambda^2 - h_1^2)}{2\lambda(s-1)\sin^2\chi\cos^2\theta} \cdot \frac{1}{m^{s-1}_{min}} \qquad (9)$$

where

$$m_{min} = B_1 \sqrt{\frac{\sigma_m R^3}{P_t \lambda^3}\,\frac{1}{G}\,\frac{\mu N}{\beta \alpha_m \lambda}\,\xi e^{(2\pi/\lambda)^2(\varepsilon^2 + \varepsilon DT_{min})}} \qquad (10)$$

$$B_1 = 1.6 \cdot 10^{14}\ \Delta T^{-1};\quad \xi = \frac{\Delta^{0.5}}{1 - e^{-1.5\Delta^{0.5}}}. \qquad (11)$$

Formulas (9) and (10) may be used as approximative operational formulas.

3. A COMPARISON OF RADAR SETS WITH DIFFERENT PARAMETERS

We will compare the number of echos registered by two radar units in a certain sector $\Delta\theta$ under equal stable conditions.

It follows from (9), (10), (11) and (5) in the case of weak diffusion ($\Delta \ll 1$) that

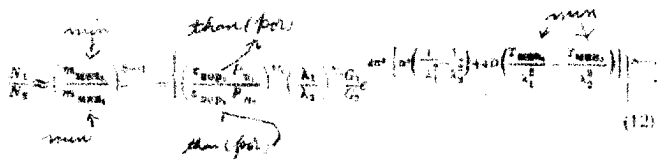

. (12)

In the case of intensive diffusion ($\Delta > 2$)

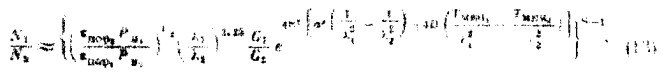

. (13)

Knowing the number of meteors registered by one of the station, we may by means of conversion determine the expected quantity of meteors discovered by another station (under analogous circumstances). It should be borne in mind that the relation N_1/N_2 will be determined by the meteor's parameters rather than by the parameters of the radar set alone, inasmuch as the values σ and D, which are determinable for a characteristic altitude, depend on the velocity of the meteoric body, the zenith distance of the radian, etc. Besides, N_1/N_2 depend on the mass distribution of the meteoric bodies.

Formulas (12) and (13) have been obtained in somewhat different form by F.I. Peregudov (4).

While examining this problem, we did not take into consideration the instance of very intensive diffusion.

Tomsk Polytechnic Institute

Submitted to the editor
3 October 1958

BIBLIOGRAPHY

1. D.W.R. McKinley: Canad. J. Phys., 29, 1951.

2. T.R. Kaiser: Advances Phys., 2, 495, 1953.

3. Ye.I. Fialko: Tr. Vsesoyuznoy konferentsii po radiofizicheskim metodam issledovaniya ionosfery [Proceedings of the All-Union Conference on Radio-Physical Methods of Investigating the Ionosphere], 1956, Tomsk, 1959.

4. F.I. Peregudov: Astron. zh. [Astronomical Journal], 35, 888, 1958.

5. Ye.I. Fialko: Izv. Tomskogo politekhn. in-ta [News of Tomsk Polytechnic Institute], 105, 1959.

6. B.Yu. Levin: Fizicheskaya teoriya meteorov i meteornoye veshchestvo v solnechnoy sisteme [The Physical Theory of Meteors and Meteoric Matter in the Solar System], Publishing House of the Academy of Sciences USSR, 1956.

OSO: 3138-N/c

A MOLECULAR TIME AND FREQUENCY STANDARD

A. Ya. Leykin

Astronomicheskiy Zhurnal
[Astronomical Journal],
Vol. XXXVI, No.4, Moscow,
Jul.-Aug. 1959, pp.734-738

A report is made on the creation of a molecular time and frequency standard at the Kharkov State Institute of Measures and Measuring Instruments, which is based on the application of a molecular generator using a beam of ammonia molecules.
A procedure is described for tuning the frequency of the molecular generator according to minimum frequency variation as a function of the ammonia pressure in the beam source. The resolving power of this tuning method is estimated at $3\ 10^{-10}$.
The first results are given of the determination of the molecular generator's frequency expressed in a second of universal time, UT-2, found from regular comparisons (beginning 5 February 1958) between the frequncies of the molecular generator and a continuously operating quartz generator of the No.3 frequncy standard of the Institute.
It is pointed out that a molecular generator employing an ammonia molecular beam together with a continuously operating quartz clock can be used successfully as a time and frequency standard.

Irregularities in the earth's rotation limit the accuracy of reproducing time and frequency units. In connection with this the need has arisen to apply a new time and frequency standard which is not bound to the earth's rotation. Atomic and molecular standards have appeared to be most appropriate for this purpose.

The absolute frequency value of these devices (these frequencies ordinarily lie in the centimeter and millimeter wavelength bands) are basically determined by atomic and molecular absorption spectra or the irradiation of matter and depend very little on external conditions. If a periodic comparison is made between atomic (or molecular) frequency standards and continuously operating quartz clocks, it becomes possible to have a time standard, unconnected with the earth's rotation. Hitherto, only microwave absorption spectra of cesium (1) have been used for systematic comparison with a continuously operating quartz clock. This device has been called the cesium resonator.

A description is given in (2) of the application of a molecular ammonia generator for this purpose, however one cannot form any concept of the systematic nature of these observations from the data presented. And, besides, the number of these observations is not very large.

A molecular generator using an ammonia beam (3), developed by N.G. Basov and A.M. Prokhorov has been employed for this purpose since February 1958 at the Khar'kov State Institute of Measures and Measuring Instruments. The electrical parameters selected for our molecular generator are the same as in (4) (the length of the quadrupole capacitor which sorts the molecules according to energy level and focusses the molecular beam is lk - 100 mm, the length of the volumetric resonator lp - 27 mm, the diameter of the resonator dp - 9.725 mm), although a number of changes have been introduced into its construction.

The resonator of the generator has been provided with a mechanical tuning system which permits a running change in generated frequency within small limits. Two independent molecular generators are mounted in a single vacuum housing. Fig.1 shows a photograph of the overall appearance of the molecular generator, also showing it with the hood removed.

As it is known, at a very high transient stability in the frequency of the molecular generator, its absolute value can change substantially as a function of the intensity of the molecular beam (the pressure of the ammonia at the beam source and voltage in the quadrupole capacitor) and, especially, as a function of the geometrical

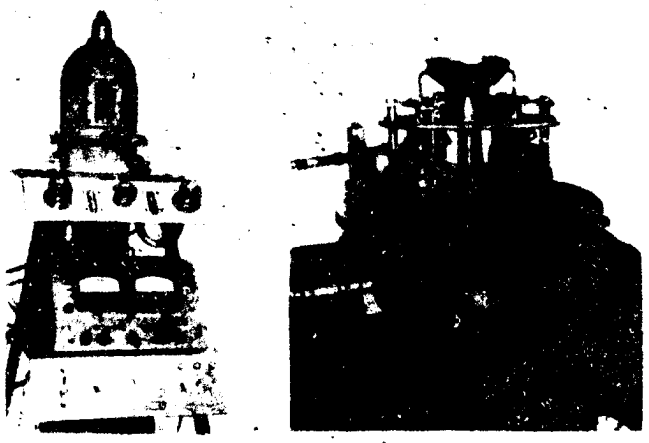

Figure 1. a - A photograph of the overall appearance of the molecular generator; b - the molecular generator with the housing removed

dimensions of the resonator (3,5). Hence, in order to use the molecular generator as a frequency standard, it has been necessary to develop this tuning method which will provide the reproduction of an absolute frequency value with great accuracy.

Investigations (6) made in 1957 have shown that for our molecular generator model the dependence of frequency on the ammonia pressure at the molecular beam source is an order larger than on the voltage in the quadrupole capacitor. At the same time, as follows from (3,5), tuning positions have also been found in the resonator for which the generator's frequency had changed very little upon variations in the amount of voltage in the quadrupole capacitor and in the ammonia pressure at the molecular beam source. Although resonator tunings which correspond to the minimum frequency change in the molecular generator as a function of ammonia pressure and voltage at the quadrupole capacitor do not coincide, it did appear that if the resonator is tuned according to the minimum frequency change from the ammonia pressure, when voltage variation in the quadrupole capacitor of 10 percent occurred, the frequency was altered by approx. $1 \cdot 10^{-10}$. This singularity was, to be sure, anticipated on the basis of the method developed for tuning the

molecular generator (6).

Its operating principle may be clarified by an examination of the block-diagram depicted in fig. 2.

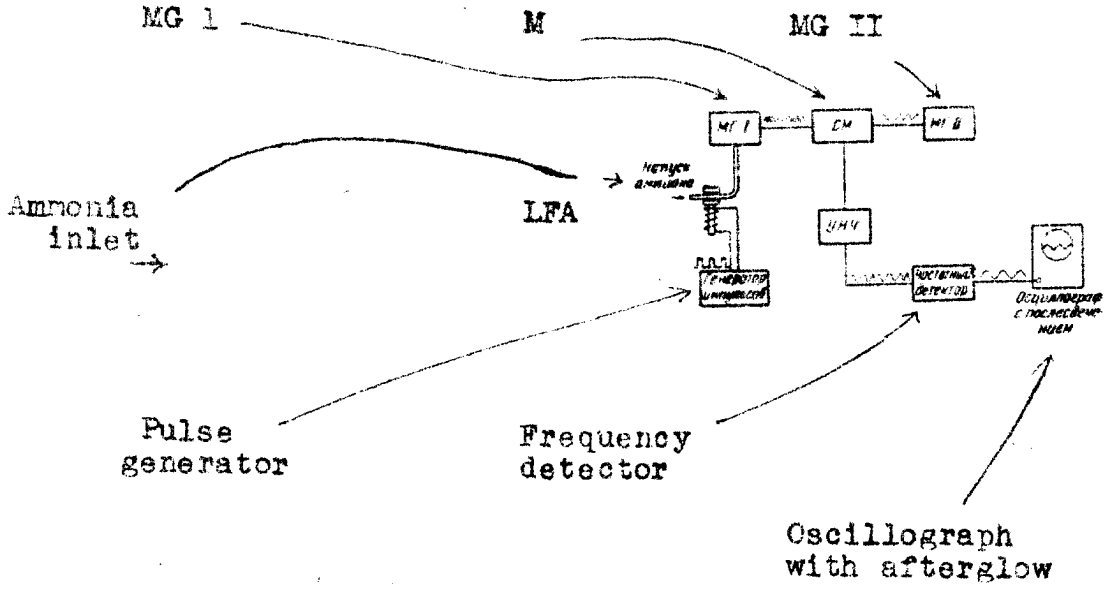

Fig. 2 Block Diagram of the molecular generator tuning system

The signals from the two molecular generators (MG I and MG II) are applied to a mixer (M). At the mixer output, difference frequency oscillations are gotten, whereupon, inasmuch as the frequencies of the generators differ somewhat, this frequency will be low (in the order of several hundred cycles per second). After amplification by the low frequency amplifier (LFA), the difference frequency oscillations are fed into the input of the frequency detector. At the output of the frequency detector, an electron oscillograph with a long-lasting afterglow screen and low velocity scanning is attached as an indicator.

It is easy enough to see that if the frequencies of the oscillations from both generators are constant or change very slowly in time, the amplitude of the voltage

at the frequency detector output will equal zero, and the beam on the oscillograph screen will draw a straight line.

We will now assume that there is a tube through which ammonia enters the molecular generator MG-I and is periodically constricted by an electromagnet regulated by the pulse generator. The ammonia pressure at the molecular beam source of the MG-I generator will then also be varied periodically, and, consequently, the frequency which it produces will also alternate. In other words, the MG-I generator's oscillations will turn out to be frequency modulated. Whereupon, the difference frequency signal (at the mixer's output) will also be frequency modulated, and alternating voltage will appear at the output of the frequency detector, the amplitude of which will be proportional to the value of the frequency change in oscillations from the MG-I generator, and the form will be traced by the beam on the oscillograph screen.

When the tuning is changed in the MG-I generator's resonator, the amplitude of the alternating voltage seen on the oscillograph screen will be altered.

A tuning position can be found for which (at a given sensitivity in the entire installation) the amplitude of the alternating voltage will equal zero, and a straight line will be seen on the oscillograph screen. This will also be the tuning position of the resonator at which the molecular generator's frequency depends very little on changes in the pressure of the ammonia, and if the slight variation in frequency from the voltage difference in the quadrupole capacitor is ignored, it will be equal (3) in the first approximation to the spectral transition frequency. The resolving power of the tuning method has the value $\sim 3 \cdot 10^{-10}$. It appears to us that this can be raised later on.

The frequency of the molecular generator, tuned in the manner described, has beginning on 5 February 1958 been systematically compared with the frequency of the quartz generator of the No.3 group frequency standard of the Institute, in continuous operation since 1950 by means of a special collation system.(6). From 8 March comparison has been made with the two molecular generators. It has turned out that the root-mean-square deviation in the difference frequency of the two molecular generators from the mean value has comprised $\pm 2.5 \cdot 10^{-10}$.

We note that in preparing the generators measures were not taken to obtain complete identity in all the elements. Moreover, certain elements have been knowingly

altered. Thus, for example, the energy factor in the resonators differ by about two times. Regardless of how the comparison findings are shown, the differences in the absolute values of their frequencies do not exceed the resolving power of the tuning method.

The frequency of the molecular generator is determined on the basis of a second of universal time, UT-2, which is based on the earth's rotation. To this end, by means of a KKhZ quartz clock measurements are taken daily of the frequency of the molecular generator according to time signals given by station GBZ at 10 hours with subsequent correction for standard time (as published).

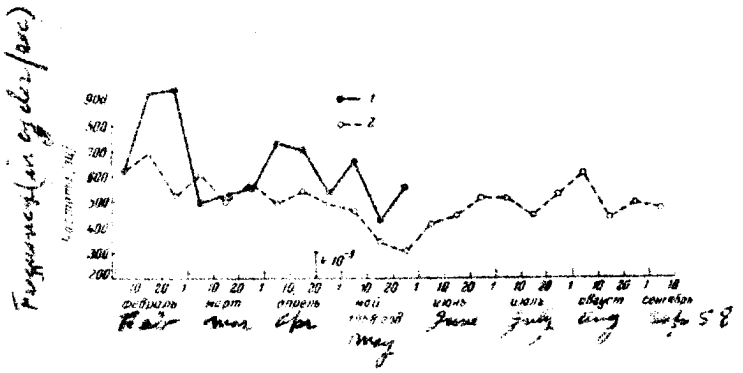

Figure 3. The frequency of the molecular generator as a function of UT-2 (according to time signal reception from station GBZ 10h. 1 - with correction for standard time; 2 - without standard time correction

Figure 3 shows the frequency of the molecular generator as a function of time. Each point is the average value of frequency calculated per ten day period. The solid line curve has been plotted with consideration of the standard time correction, while the broken line has not been adjusted and is drafted only according to time signal reception. In view of the great accuracy in reproducing the absolute value of frequency in the molecular generator, the scattering of points indicates inaccuracy in the reception of the time signals.

Performing the comparisons described makes it possible in the future, it appears to us, to obtain data on non-periodic variations in the rotational velocity of the earth, similar to those shown in (7).

It follows from an examination of the findings that the molecular generator using an ammonia molecule beam, together with a continuously operating quartz clock, can be successfully utilized as a time and frequency standard. It therefore seems to us that Essen's (8) claim that the ammonia standard is less accurate than cesium is premature.

In conclusion we will take this opportunity to extend our thanks to L.D. Bryzzhev for his unflagging interest in this work, his valuable counsel and judgment on the findings.

In preparing the molecular generator, developing the collation system and making comparison checks, Ye. Z. Orlov, A.I. Samoylovich, I.V. Baulin and M.I. Klyus have been collaborators. The author expresses his thanks to them.

Khar'kov State Institute
of Measures and Measuring
Instruments

Submitted to
the editor
12 September 1958

BIBLIOGRAPHY

1. L. Essen, J.V.L. Parry: Nature, 176, 280, 1955; Philos. Trans. Roy. Soc., London, 250, 45, 1957.

2. I. Bonanomy, J. Prince, J. Hermann, P. Kartaschoff: Helv. Phys. Acta, 30, 288, 1957.

3. N.G. Basov and A.M. Prokhorov: Uspekhi fiz. nauk [Achievements of the Physical Sciences], 7, 485,1955.

N.G. Basov. Dissertatsiya [Dissertation]. Fizicheskiy Inst. AN SSSR im. P.N. Lebedeva, 1956.

4. N.G. Basov Radiotekhnika i elektronika [Radio Engineering and Electronics], 722, 1956.

5. Gordon, Zeiger and Townes: Phys.Rev., 99, 1264, 1955

6. A.Ya.Leykin. Doklad Vsesoyuznoy nauchnoy sessii, po-

svyashchennoy dnyu radio [Report to the All-Union Scientific Session on Radio Day], May 1958, Moscow.

7. L. Essen, J.V.L. Parry, Wm. Marcovitz, R.G. Hall: Nature, 181, 1054, 1958.

8. Essen: Doklad na X Mezhdunarodnom astronomicheskom s"yezde [Report to the Tenth International Astronomical Session], August, 1958, Moscow.

THE END

#1471

CSO: 3138-N/d

OBSERVATION OF THE CRAB NEBULA WITH THE LARGE RADIO TELESCOPE OF THE MAIN ASTRONOMICAL OBSERVATORY AT PULKOVO

G.P. Apushkinskiy
Yu.N. Pariyskiy

Astronomicheskiy Zhurnal
[Astronomical Journal],
Vol. XXXVI, No.4, Moscow,
Jul.-Aug. 1959, pp.739-740.

The results of preliminary observation of the Crab Nebula on the 3 cm wave length are given. The observations were made at Pulkovo Observatory with a radio telescope of high resolving power.
The angular dimensions, the coordinates of the active center of radio emission and the asymmetry of the source were determined.

The findings are discussed of preliminary observations made in September 1958 on the wave $\lambda=3$ cm, with a radio telescope (1) having a beavertail beam approximately 2' X 20' in size with a receiver (2) having a sensitivity of 0.2° K at constant time $\tau=2.5$ sec.

Three recordings were made of transmissions from the source through the antenna pattern, laid out on a large scale in the meridian plane.

Fig. 1 shows the recording averaged by the four

transmissions (the dash-line curve is given, plotted symmetrically to the eastern edge).

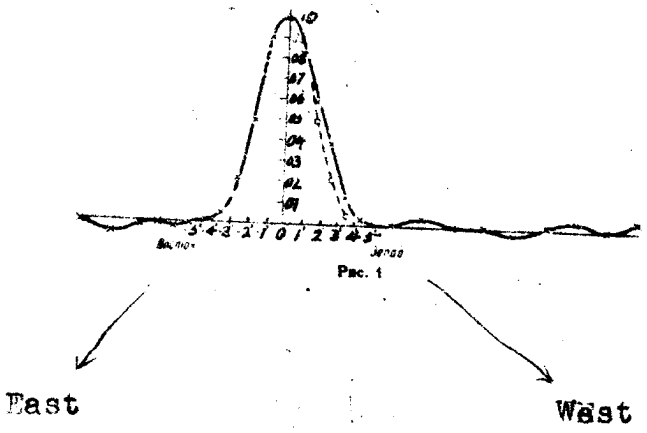

Figure 1

The half-width and limits of the radio-emission area of the source, adjusted to the antenna pattern were 3'.4±0'.1 and less than 6', respectively. Asymmetry was noticeable; the western edge was at a greater slant which qualitatively coincided with eclipse observations at wave length λ=75 cm (3).

The coordinate of the active emission center in right ascension was $\alpha_{1950} = 5^h\ 31^m\ 29^s,55 \pm 1^s$.

It is interesting to note that the emission center has shifted west of the former supernovae toward the great cluster (see, for example (4). It is possible that this displacement has been caused by the asymmetry of the source.

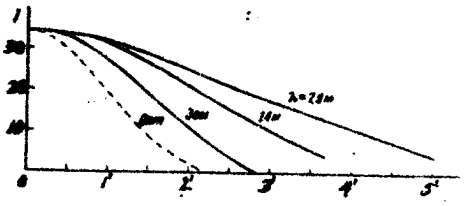

Fig. 2

A comparison is given in fig. 2 of the distribution of radio brightness with observations in the optical and radio wave ranges (4,5,6). It has recently been proposed at the Main Astronomical Observatory that a detailed study of the Crab Nebula be conducted with a greater resolving power.

Main Astronomical Observatory
Academy of Sciences USSR

Submitted to the
editor 17 March 1959

BIBLIOGRAPHY

1. S.E. Khaykin, N.L. Kaydanovskiy. Zh. pribory i tekhnika eksperimenta [Journal of Experimental Instrumentation and Technology], No. 2, 1959.

2. G.P. Apushkinskiy. Radiotekhnika i elektronika [Radio Engineering and Electronics], No. 6, 1958.

3. Ch.L. Seger, G. Westerhout: Bull. Astron. Inst. Netherl., XIII, 312,1957.

4. I.S. Shklovskiy. Kosmicheskoye radioizlucheniye [Cosmic Radio Emission], Moscow, 1956.

5. B.Y. Mills: Austr. J. Phys., 6, 452, 1952.

6. G.H. Costain, B. Elsmore, G.R. Whitfield: Monthly Notices, 116, No.4, 1956.

END

#1471